

A Polymer-Coated Rhodium/Diamine-Functionalized Silica for Controllable Reaction Switching in Enantioselective Tandem Reduction–Lactonization of Ethyl 2-Acylarylcarboxylates

Lingyu Kong, Junwei Zhao, Tanyu Cheng, Jingrong Lin, and Guohua Liu*

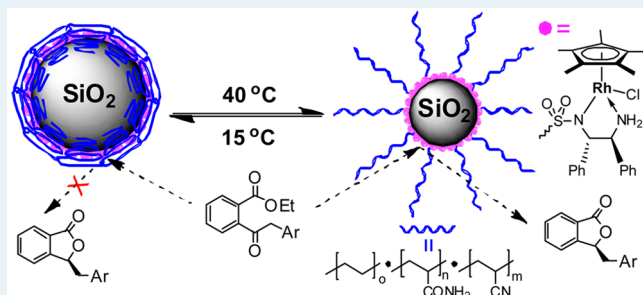
Key Laboratory of Resource Chemistry of Ministry of Education, Shanghai Key Laboratory of Rare Earth Functional Materials, Shanghai Normal University, Shanghai 200234, China

Supporting Information

ABSTRACT: The design of a smart heterogeneous catalyst for controllable reaction switching is highly desirable in asymmetric catalysis. In this work, by taking advantage of the thermoresponsive behavior of a water-soluble polymer coating and the confined feature of silica nanoparticles, we have constructed a silica material with chiral rhodium/diamine functionality on SiO₂ nanospheres coated with a water-soluble thermoresponsive polymer. The solid-state ¹³C NMR spectrum of the product demonstrated well-defined single-site chiral rhodium active centers within the thermoresponsive polymer, and scanning electron microscopy and transmission

electron microscopy revealed its uniformly dispersed morphology. As a smart heterogeneous catalyst, it enables catalyst-based temperature-controlled reaction switching in the enantioselective tandem reduction–lactonization of ethyl 2-acylarylcarboxylates in water. At 40 °C, the catalyst promotes highly enantioselective tandem reduction–lactonization by adopting the extended form of the thermoresponsive polymer coating, whereas at 15 °C the reaction is terminated and the heterogeneous catalyst can be recycled because of its closed form. This feature endows this catalyst with high efficiency and recyclability for the synthesis of chiral phthalides in an environmentally friendly medium.

KEYWORDS: asymmetric catalysis, heterogeneous catalyst, immobilization, silica, polymer



INTRODUCTION

Thermoresponsive polymers show a reversible response to temperature, whereupon their properties can be drastically altered with changes in temperature.¹ This feature is beneficial for the design of a polymer-based smart heterogeneous catalyst for controllable reaction switching based on temperature, which has not been explored to date. Generally, two types of polymer-based heterogeneous catalysts have been applied to catalytic reactions,² namely, polymer-supported catalysts (homogeneous complexes supported on polymers) and polymer-encapsulated catalysts (homogeneous complexes encapsulated within polymers). However, both cases have some intrinsic shortcomings. In the case of polymer-supported catalysts, the active species are randomly bound to a polymer, making it impossible for this polymer to completely entrap these active species within its interior, and therefore, it is difficult to rigorously regulate its catalytic behavior.^{2a,3} As a result, it is not feasible to achieve reaction switching by exploiting the extended and closed forms of a thermoresponsive polymer. In the case of polymer-encapsulated catalysts, loss of active species from the extended form of a thermoresponsive polymer is unavoidable during the catalytic process.^{2b,c} Therefore, the development of a thermoresponsive-polymer-based catalyst to overcome these limitations and the realization of real catalyst-based temper-

ature-controlled reaction switching are key scientific and technological challenges in heterogeneous asymmetric catalysis.

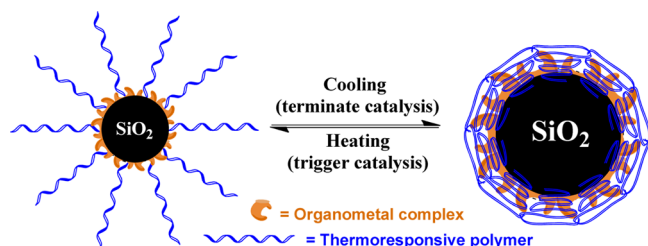
Recently, chiral organometallic complexes immobilized on silica-based supports have been extensively applied to various asymmetric reactions.⁴ A significant benefit of this method is that a homogeneous chiral organometallic complex is efficiently confined on its support, avoiding loss of its catalytically active species. Furthermore, unlike polymer-based catalysts,⁵ relatively rigid silica-based supports can overcome the negative influence on enantioselectivity that arises from the flexible nature and the swelling effect of soluble polymers, resulting in comparable enantioselective performance.⁶ Thus, by the combination of the reversible temperature responsiveness of a thermoresponsive polymer and the confining effect of silica nanoparticles, it is reasonable to expect that a thermoresponsive-polymer-coated chiral organometal-functionalized silica may serve as a smart catalyst to perform controllable reaction switching based on temperature (Scheme 1).

Our recent efforts have indicated that silica-based catalysts can maintain highly enantioselective performance in asym-

Received: December 10, 2015

Revised: February 22, 2016

Scheme 1. Schematic Illustration of the Reversible Response to Temperature of a Polymer-Coated Organometal-Functionalized Silica for Controllable Catalysis



metric reactions.⁷ In this work, by combining the benefits of a thermoresponsive polymer and silica nanoparticles, we have constructed a thermoresponsive-polymer-coated rhodium/diamine-functionalized silica material as a smart heterogeneous catalyst. This catalyst enables controllable reaction switching in the enantioselective tandem reduction–lactonization of ethyl 2-acrylylcarboxylates in water. At 40 °C, the polymer coating is in an extended form, allowing the asymmetric reaction to proceed with high catalytic efficiency because of the homogeneous-like catalytic environment. At 15 °C, however, the polymer coating is converted to the closed form, terminating the reaction, and the catalyst can be efficiently recycled. Moreover, the catalyst displays an enhanced reaction rate and comparable enantioselective performance relative to its homogeneous counterpart, which can be attributed to the water-soluble polymer coating and the confined chiral rhodium/diamine catalyst. Furthermore, the heterogeneous catalyst can be recycled at least eight times without loss of its enantioselective performance.

EXPERIMENTAL SECTION

Preparation of Vinyl@ArDPEN@SiO₂ (2). In a typical synthesis, the obtained SiO₂ nanospheres were treated before use as follows. The nanospheres were immersed in a 1.0% HCl solution for 8 h at room temperature to remove contaminants, followed by washing and immersion in deionized water for approximately 1 h to clean and hydrolyze the surface. The nanospheres were then filtered and dried at 110 °C in a vacuum oven overnight to remove excess surface water, affording clean hydroxylated SiO₂ nanospheres. Subsequently, 2.0 g of the hydroxylated SiO₂ nanospheres was added to a solution of 0.20 g (0.40 mmol) of (*S,S*)-4-((trimethoxysilyl)ethyl)phenylsulfonyl-1,2-diphenylethylenediamine (**1**) in 20 mL of xylene, and the mixture was stirred at room temperature for 1 h, refluxed at 137 °C for 12 h, and cooled to room temperature. Then 0.40 g (2.10 mmol) of triethoxy(vinyl)silane was added, and the mixture was stirred at room temperature for another 1 h and then at 70 °C for 12 h. The resulting solid was filtered, rinsed with excess xylene, and then dried at 110 °C in a vacuum oven for 2 days to afford **2** (2.49 g) in the form of a white powder.

Preparation of Catalyst 3. In a typical synthesis, 2.0 g of **2**, 1.02 g (14.4 mmol) of acrylamide, and 0.19 g (3.6 mmol) of acrylonitrile were weighed into a 100 mL nitrogen flask and dissolved in 20 mL of distilled dimethyl sulfoxide (DMSO). Then 65.5 mg (2% mol) of 2,2-azobis(isobutyronitrile) (AIBN) was added at room temperature. After a degassing process involving three freeze–pump–thaw cycles, the flask was placed into an oil bath for polymerization at 60 °C for 6.0 h. The resulting solid was filtered and then rinsed with 10.0 mL of

DMSO solvent three times and with 10.0 mL of methanol three times. The collected solid was suspended in 20 mL of deionized H₂O, and 0.12 g (0.20 mmol) of [Cp**RhCl*₂]₂ was added. The resulting mixture was stirred at 40 °C for 12 h. The resulting solids were filtered, rinsed with excess distilled H₂O, and washed with excess CH₂Cl₂. After Soxhlet extraction in CH₂Cl₂ solvent for 24 h to remove the remaining [Cp**RhCl*₂]₂, the solid was dried at 60 °C under reduced pressure overnight to afford catalyst **3** (2.58 g) as a light-yellow powder. Inductively coupled plasma (ICP) analysis showed that the Rh loading was 9.15 mg (0.089 mmol) per gram of catalyst. IR (KBr) cm⁻¹: 3421.5 (s), 3028.1 (w), 2933.6 (w), 2862.7 (w), 1628.4 (m), 1494.6 (w), 1455.3 (w), 1101.1 (s), 951.6 (w), 802.1 (m), 691.8 (w), 668.3 (w), 565.9 (w), 471.5 (m). ¹³C CP/MAS NMR (161.9 MHz): 179.1 (C=O), 146.9, 138.1, 128.0 (C of Ar and Ph and –CN), 95.3 (–CH of Cp ring), 75.1, 70.1 (–NCHCHN–), 66.9–56.4 (–OCH₂CH₃), 49.6–22.8 (–CH₂CH₂–, –CH₂CONH₂, and –CH₂Ar), 16.9 (CH₃CH₂–, and –OCH₂CH₃), 9.2 (–CH₃Cp, –CH₂Si) ppm.

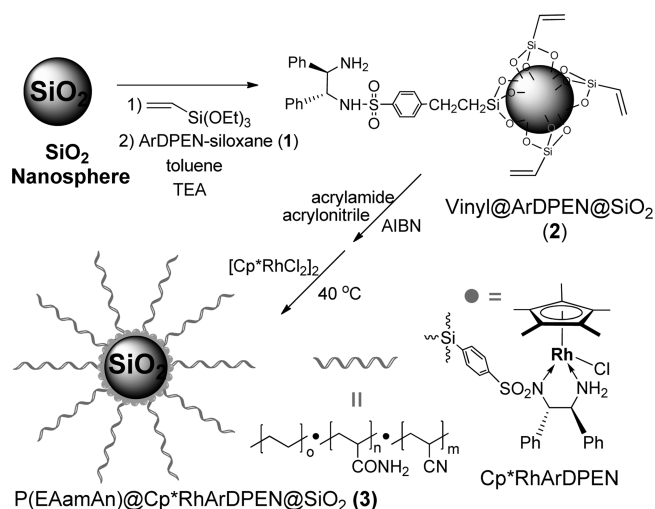
General Procedure for the Enantioselective Tandem Reduction–Lactonization of Ethyl 2-Acrylylcarboxylates. A typical procedure was as follows: The heterogeneous catalyst **3** (22.50 mg, 2.0 μmol of Rh based on ICP analysis), HCO₂Na (1.0 mmol), 2-acrylylcarboxylate (0.20 mmol), and 2.0 mL of water were added to a 10 mL flask, which in turn was purged with nitrogen. The mixture was allowed to react at 40 °C for 8–12 h. During that time, the reaction was monitored constantly by thin-layer chromatography. After completion of the reaction, the heterogeneous catalyst was separated from the mixture via centrifugation (10000 rpm) for the recycle experiment. The aqueous solution was extracted with Et₂O (3 × 3.0 mL). The combined Et₂O was washed with brine twice and dried with Na₂SO₄. After evaporation of the Et₂O, the residue was purified by silica gel flash column chromatography to afford the desired product. The yields were determined by ¹H NMR analysis, and the ee values were determined by HPLC analysis with a photodiode array detector using a Daicel Chiralcel column (Φ = 0.46 cm × L = 25 cm).

RESULTS AND DISCUSSION

Synthesis and Structural Characterization of Heterogeneous Catalyst 3. Water-soluble thermoresponsive-polymer-coated Cp**RhArDPEN*-functionalized silica, abbreviated as P(EAmAn)@Cp**RhArDPEN*@SiO₂ (**3**), [P(EAmAn)⁸ = poly(ethene-*co*-acrylamide-*co*-acrylonitrile); Cp**RhArDPEN*:⁹ Cp* = pentamethylcyclopentadiene, ArDPEN = (*S,S*)-4-((trimethoxysilyl)ethyl)phenylsulfonyl-1,2-diphenylethylenediamine (**1**)], was prepared as outlined in Scheme 2. First, SiO₂ nanospheres were obtained through condensation of tetraethoxysilane according to the reported method.¹⁰ Continuous postgraftings of triethoxy(vinyl)silane and **1** then afforded Vinyl@ArDPEN@SiO₂ (**2**).¹¹ Finally, the free radical polymerization of **2** with acrylamide and acrylonitrile¹² followed by complexation with [Cp**RhCl*₂]₂ at 40 °C led to catalyst **3** in the form of a light-yellow powder (see the the experimental section and Figure S1 in the Supporting Information). For comparison, a parallel polymer-supported analogue without the SiO₂ support, P(EAmAn)@Cp**RhArDPEN* (**3'**), was also prepared by free radical polymerization of *N*-((*S,S*)-2-amino-1,2-diphenylethyl)-4-vinylbenzenesulfonamide with acrylamide and acrylonitrile following a similar procedure.

Incorporation of single-site rhodium active species in the polymer-coated SiO₂ nanospheres was proved by solid-state

Scheme 2. Preparation of Heterogeneous Catalyst 3



¹³C cross-polarization/magic-angle spinning (CP/MAS) NMR spectroscopy. As shown in Figure 1, catalyst 3 produced strong

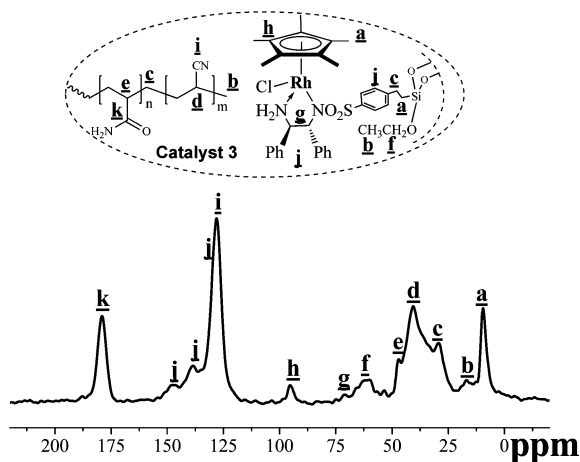


Figure 1. Solid-state ¹³C CP/MAS NMR spectrum of catalyst 3.

carbon signals of the $-\text{CHCONH}_2$ moiety at $\delta = 179.1$ ppm and the $-\text{CHCN}$ moiety at $\delta = 128.0$ ppm, corresponding to the characteristic carbon atoms of the coated polymer.¹³ In addition, strong signals for the alkyl carbon atoms of the coated polymer could be observed, as marked in the spectrum. In particular, all of the carbon atoms of the chiral rhodium/diamine complex showed their characteristic signals. Specifically, the signals between $\delta = 70$ and 75 ppm could be attributed to the NCHPh carbon atoms in the ArDPEN moiety, and the peaks at $\delta = 95.3$ and 9.2 ppm could be ascribed to the carbon atoms of the Cp ring and the attached CH_3 groups, respectively. These chemical shifts of catalyst 3 are similar to those of the homogeneous counterpart, $\text{Cp}^*\text{RhTsDPEN}$,¹⁴ demonstrating that both have the same well-defined single-site active species. Similarly, the parallel polymer-supported catalyst 3' also showed the same chemical shifts in its ¹³C CP/MAS NMR spectrum (see Figure S2), suggesting that it could be regarded as a standard analogue for comparison of catalytic performances.

The nanostructural morphology of catalyst 3 was further investigated by means of scanning electron microscopy (SEM) and transmission electron microscopy (TEM). As shown in

Figure 2, SEM images revealed that catalyst 3 was composed of uniformly dispersed nanospheres with an average diameter of

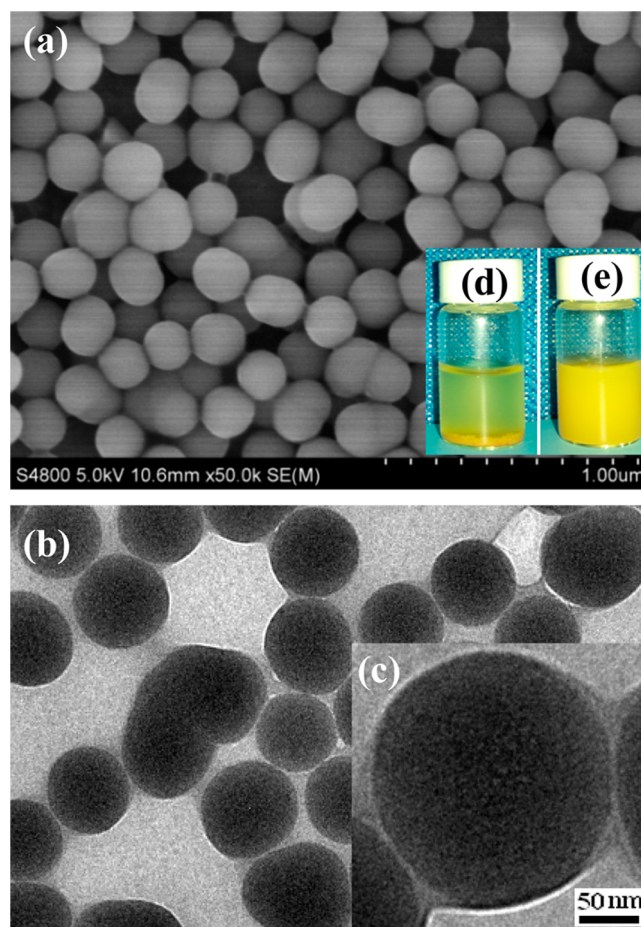
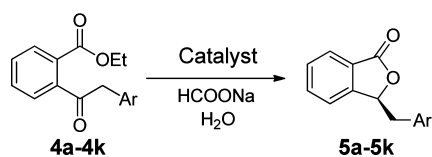


Figure 2. (a) SEM image, (b) TEM image, and (c) enlarged TEM image of catalyst 3 and (d, e) photographs showing dispersions of catalyst 3 in water at (d) 15 °C and (e) 40 °C.

347 nm (Figure 2a), while TEM images confirmed that these nanospheres had a core-shell structure in which the core was coated by a polymer shell with a thickness of about 15 nm (Figure 2b,c). It is noteworthy that catalyst 3 could be better dispersed in water at 40 °C than at 15 °C (cf. Figure 2d,e), suggesting that it adopted its extended form at the higher temperature and its closed form at the lower temperature.

Catalytic Property of the Heterogeneous Catalyst.

Chiral N-sulfonylated diamine-based organometallic complexes are extensively used for various asymmetric reactions, and some of them have been applied to the enantioselective reduction-lactonization of ethyl 2-acylarylcarboxylates.^{7a,15} In the present study, we first examined the catalytic activity and enantioselectivity of 3 toward the enantioselective tandem reduction-lactonization of ethyl 2-(2-phenylacetyl)benzoate as a model reaction, where the reaction with HCO_2H as a hydrogen source and 1.0 mol % 3 as a catalyst was investigated according to a reported method.^{7a} It was found that catalyst 3 produced the target product (*S*)-3-benzylisobenzofuran-1(3*H*)-one in quantitative yield with 98% ee after 10 h. This ee value is comparable to that achieved with the homogeneous catalyst (Table 1, entry 1 vs entry 1 in parentheses). This behavior indicated that the $\text{Cp}^*\text{RhArDPEN}$ functionality appended onto the SiO_2 nanospheres of catalyst 3 retained the original chiral environment of

Table 1. Enantioselective Tandem Reduction–Lactonization of Ethyl 2-Acylarylcarboxylates^a

entry	Ar	time (h)	yield (%) ^b	ee (%) ^b
1	Ph (5a)	10 (24)	99 (97)	98 (96) ^c
2	Ph (5a)	48	8	85 ^d
3	Ph (5a)	48	85	95 ^e
4	Ph (5a)	48	63	93 ^f
5	Ph (5a)	8	98	94 ^g
6	4-FPh (5b)	12	99	99
7	4-ClPh (5c)	12	99	99
8	2-ClPh (5d)	14	98	98
9	4-CF ₃ Ph (5e)	12	99	98
10	4-MePh (5f)	14	97	99
11	4-MeOPh (5g)	14	98	96
12	3-MeOPh (5h)	14	97	99
13	3,4-(MeO) ₂ Ph (5i)	14	93	99
14	1-naphthyl (5j)	14	97	98
15	2-naphthyl (5k)	14	98	99

^aReaction conditions: catalyst 3 (22.50 mg, 2.0 μ mol of Rh based on ICP analysis), HCO₂Na (1.0 mmol), ethyl 2-acylarylcarboxylate (0.20 mmol), and 2.0 mL water at the reaction temperature (15 °C in entries 2 and 3 and 40 °C in the others). ^bYields were determined by ¹H NMR analysis (see Figure S5) and ee values by chiral HPLC analysis (see Figure S6). ^cData in parentheses were obtained using homogeneous Cp^{*}RhTsDPEN as the catalyst. ^dData were obtained at 15 °C using 3 as the catalyst. ^eData were obtained at 15 °C using homogeneous Cp^{*}RhTsDPEN as the catalyst. ^fData were obtained using 3' as the catalyst at 15 °C. ^gData were obtained using 3' as the catalyst at 40 °C.

the homogeneous analogue and led to a similar enantioselective performance, further confirming retention of the same well-defined single-site Cp^{*}RhArDPEN active species, as indicated by ¹³C CP/MAS NMR spectroscopy. Upon comparison of the enantioselective performances of catalyst 3 and its polymeric analogue 3', it was found that the asymmetric reaction catalyzed by 3 had a higher ee than that attained with 3', although the latter had a shorter reaction time (98% ee vs 94% ee, 10 h vs 8 h; entries 1 and 5). This difference indicated that the designed catalyst 3 could overcome the disadvantage of its polymeric analogue in terms of enantioselective performance because the flexible nature of polymer-supported analogue 3' affects the chiral environment of the active species and thereby results in a lower ee value.

On the basis of the above excellent results, heterogeneous catalyst 3 was further investigated with a series of substrates in the enantioselective tandem reduction–lactonization. As shown in Table 1, all of the tested substrates were smoothly transformed to the corresponding chiral phthalides in high yields with excellent enantioselectivities (>96% ee). Also, it was found that the structures and electronic properties of substituents on the Ar moiety did not affect the enantioselectivity, as various electron-withdrawing and -donating substituents on the Ar moiety were equally efficient (entries 6–15). This behavior mirrors that attained with its homogeneous counterpart,^{15a} suggesting that during the catalytic process at 40 °C the heterogeneous catalyst 3 adopted

the extended form of its water-soluble polymer coating. As a result, the Cp^{*}RhArDPEN functionality appended onto the SiO₂ nanospheres was fully exposed to the reaction system, leading to a homogeneous-like catalytic environment for the active centers and hence the same catalytic behavior in its catalytic performance. The consistency of the results also implied that the extended form of the water-soluble polymer coating in catalyst 3 did not disturb the configuration of the Cp^{*}RhArDPEN active centers during the catalytic process at 40 °C, resulting in similar enantioselectivities. Thus, heterogeneous catalyst 3 retained structural and electronic properties similar to those of its homogeneous counterpart, enabling the same catalytic and enantioselective performance in the asymmetric reaction.

To gain better insight into the nature of the catalyst-based temperature-controlled reaction switching, the tandem reduction–lactonization of ethyl 2-(2-phenylacetyl)benzoate catalyzed by 3 at 15 °C was performed. It was found that only an 8% yield of (*S*)-3-benzylisobenzofuran-1(3*H*)-one could be obtained, even when the reaction time was prolonged to 48 h (Table 1, entry 2). This yield was obviously much lower than that of 99% obtained at 40 °C (entry 1) and even lower than that of 85% obtained with the homogeneous counterpart Cp^{*}RhArDPEN at 15 °C (entry 3). These findings implied that the water-soluble thermoresponsive polymer coating of catalyst 3 at 15 °C was in its closed form because the reaction at 15 °C only afforded a small amount of product. The very low yield at 15 °C relative to that attained at 40 °C (8% vs 99% yield) should be due to the fact that the closed polymer coating greatly restricted the attack of ethyl 2-(2-phenylacetyl)benzoate to the Cp^{*}RhArDPEN active species. As a result, it was difficult for the reaction to proceed at 15 °C, and thus, a very poor yield was obtained. Further evidence supporting this view was provided by the parallel experiment, where the reaction catalyzed by the polymeric analogue 3' at 15 °C produced (*S*)-3-benzylisobenzofuran-1(3*H*)-one in 63% yield (entry 4 vs entry 2). The obviously higher yield obtained with catalyst 3' at 15 °C not only confirmed the closed nature of 3 at this temperature but also indicated that the general polymeric analogue 3' was not amenable to catalyst-based temperature-controlled reaction switching. On the other hand, the extended form of smart catalyst 3 could also be proven easily by a similar method, where the asymmetric reactions catalyzed by 3 and 3' at 40 °C both reached catalytic completion within 10 h (entries 1 and 5) because they had the similar extended form of the thermoresponsive polymer at 40 °C.

More importantly, direct evidence to detect the extended and closed forms of the polymer coating in catalyst 3 could also be offered by an investigation of the hydrodynamic diameter (*D*_h) distributions at 15 and 35 °C using dynamic laser scattering (DLS). As shown in Figure 3, catalyst 3 exhibited steady temperature responsiveness over five consecutive runs, where the average *D*_h increased from 347 to 427 nm as the temperature was increased from 15 to 35 °C (also see Figure S4). In sharp contrast with original average size of catalyst 3 at 15 °C (average diameter 347 nm with a coated layer thickness of 15 nm as determined by SEM and TEM), the increase in the average diameter (50 nm) at 40 °C [average diameter at 40 °C (427 nm) – average diameter at 15 °C (347 nm) – twice the polymer coating thickness (2 × 15 nm)] should be ascribed to the extended length of the polymer coating. These observations confirmed the adoption of the extended and closed forms of the polymer coating in catalyst 3, as differential scanning

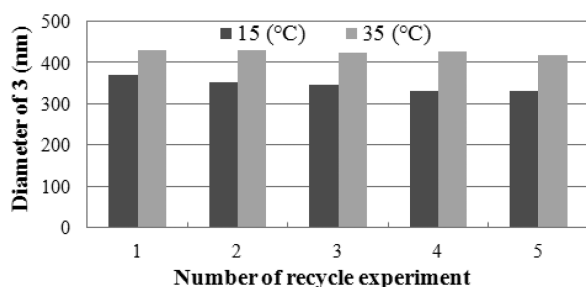


Figure 3. Average hydrodynamic diameter distributions of catalyst 3 at 15 and 35 °C in water.

calorimetry analysis showed that the melting point of catalyst 3 was 168 °C (see Figure S3).^{12b}

It is noteworthy that the asymmetric reaction catalyzed by 3 proceeded rapidly in the absence of Bu₄NBr, reaching completion within 10 h, whereas the reaction required 24 h with its homogeneous counterpart Cp*RhArDPEN (Table 1, entry 1 versus entry 1 in parentheses). This behavior is rare in this tandem asymmetric reaction because Bu₄NBr is necessary to promote the catalytic performance in a homogeneous catalysis system. This observation demonstrated that the extended polymer coating in catalyst 3 at 40 °C could play a similar role as Bu₄NBr in the homogeneous catalytic system, greatly promoting the catalytic performance. In order to elucidate the role of the polymer coating during the catalytic process, parallel reactions at 40 °C were compared through kinetic profiles of the enantioselective tandem reduction–lactonization of ethyl 2-(2-phenylacetyl)benzoate catalyzed by 3 in the absence of Bu₄NBr and catalyzed by Cp*RhArDPEN in the presence or absence of Bu₄NBr. As shown in Figure 4,

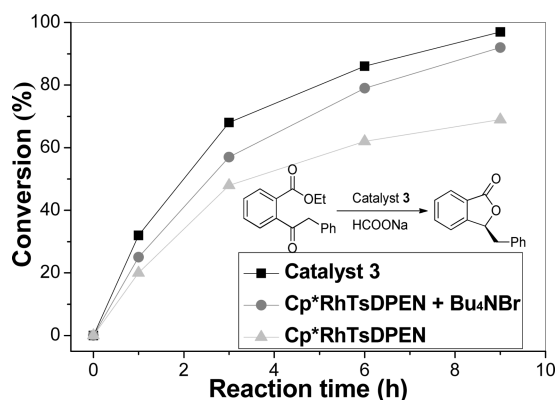


Figure 4. Comparison of the kinetic profiles for the enantioselective tandem reduction–lactonization of ethyl 2-(2-phenylacetyl)benzoate catalyzed by 3 in the absence of Bu₄NBr and catalyzed by Cp*RhArDPEN in the presence or absence of Bu₄NBr. Reactions were carried out at substrate-to-catalyst mole ratio of 200.

the initial turnover frequency (TOF) values were 64, 50, and 40 mol mol⁻¹ h⁻¹, respectively (TOF = number of moles of substrate converted per mole of catalyst per hour). The results confirmed that the enhanced reaction rate attained with 3 at 40 °C could be attributed to its highly dispersed nature (Figure 2e) because of its extended water-soluble polymer coating.

Another important consideration concerns the ability to recycle the heterogeneous catalyst through this catalyst-based temperature-controlled reaction switching. As observed, the asymmetric reaction could be terminated easily and catalyst 3

recovered conveniently by simple centrifugation. As shown in Figure 5, in eight consecutive recycles, catalyst 3 still afforded

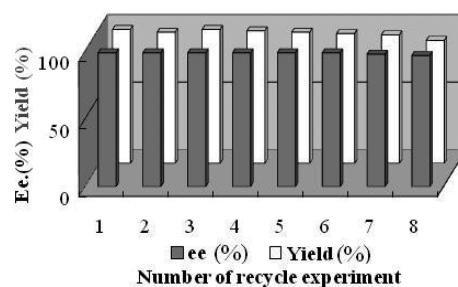


Figure 5. Reusability of catalyst 3 for the tandem reduction–lactonization of ethyl 2-(2-phenylacetyl)benzoate.

the desired products in 91% yield with 97% ee in the enantioselective reduction–lactonization of ethyl 2-(2-(4-bromophenyl)acetyl)benzoate (see Table S1 and Figure S7). Importantly, the closed form of the water-soluble polymer coating in catalyst 3 efficiently decreased the leaching of Rh, as only 3.6% of the Rh had been lost after the eighth recycle as determined by ICP optical emission analysis.

In conclusion, by taking advantage of the thermoresponsive behavior of a water-soluble polymer coating and the confining effect of SiO₂ nanoparticles, we have constructed a smart heterogeneous catalyst that enables catalyst-based temperature-controlled reaction switching in the enantioselective tandem reduction–lactonization of ethyl 2-acylarylcarboxylates in water. The extended form of the polymer coating of catalyst 3 at 40 °C facilitates highly efficient tandem asymmetric catalysis, whereas the closed form at 15 °C terminates the reaction. The heterogeneous catalyst could be easily recovered and reused repeatedly at least eight times without loss of enantioselectivity. The highly dispersed extended polymer coating and the confined chiral rhodium/diamine catalytic centers combined to further boost the catalytic performance. The work described here offers a new concept for catalyst-based temperature-controlled reaction switching that may potentially be applied to other asymmetric reactions.

■ ASSOCIATED CONTENT

📄 Supporting Information

The Supporting Information is available free of charge on the ACS Publications website at DOI: 10.1021/acscatal.5b02797.

Experimental procedures and analytical data for chiral products (PDF)

■ AUTHOR INFORMATION

✉ Corresponding Author

*Tel: + 86 21 64322280. E-mail: ghliu@shnu.edu.cn.

📝 Notes

The authors declare no competing financial interest.

■ ACKNOWLEDGMENTS

We are grateful to the National Natural Science Foundation of China (21402120), the Shanghai Sciences and Technologies Development Fund (13ZR1458700), and the Shanghai Municipal Education Commission (14YZ074, 13CG48, Young Teacher Training Project) for financial support.

REFERENCES

- (1) (a) Aseyev, V.; Tenhu, H.; Winnik, F. M. *Adv. Polym. Sci.* **2010**, *242*, 29–89. (b) Theato, P.; Sumerlin, B. S.; O'Reilly, R. K.; Epps, T. H., III *Chem. Soc. Rev.* **2013**, *42*, 7055–7056. (c) Lee, H. I.; Pietrasik, J.; Sheiko, S. S.; Matyjaszewski, K. *Prog. Polym. Sci.* **2010**, *35*, 24–44. (d) Hu, J.; Liu, S. *Macromolecules* **2010**, *43*, 8315–8330. (e) Weber, C.; Hoogenboom, R.; Schubert, U. S. *Prog. Polym. Sci.* **2012**, *37*, 686–714. (f) Kryuchkov, V. A.; Daigle, J. C.; Skupov, K. M.; Claverie, J. P.; Winnik, F. M. *J. Am. Chem. Soc.* **2010**, *132*, 15573–15579.
- (2) (a) Zayas, H. A.; Lu, A.; Valade, D.; Amir, F.; Jia, Z. F.; O'Reilly, R. K.; Monteiro, M. J. *ACS Macro Lett.* **2013**, *2*, 327–331. (b) Li, G. L.; Xu, L. Q.; Neoh, K. G.; Kang, E. T. *Macromolecules* **2011**, *44*, 2365–2370. (c) Beija, M.; Marty, J. D.; Destarac, M. *Chem. Commun.* **2011**, *47*, 2826–2828. (d) Yan, N.; Zhang, J. G.; Yuan, Y.; Chen, G. T.; Dyson, P. J.; Li, Z. C.; Kou, Y. *Chem. Commun.* **2010**, *46*, 1631–1633. (e) Beija, M.; Palleau, E.; Sistach, S.; Zhao, X.; Ressler, L.; Mingotaud, C.; Destarac, M.; Marty, J. D. *J. Mater. Chem.* **2010**, *20*, 9433–9442.
- (3) (a) Foster, E. J.; Berda, E. B.; Meijer, E. W. *J. Am. Chem. Soc.* **2009**, *131*, 6964–6966. (b) Mes, T.; van der Weegen, R.; Palmans, A. R. A.; Meijer, E. W. *Angew. Chem., Int. Ed.* **2011**, *50*, 5085–5089. (c) Lightfoot, M. P.; Mair, F. S.; Pritchard, R. G.; Warren, J. E. *Chem. Commun.* **1999**, 1945–1946. (d) Smulders, M. M. J.; Schenning, A. P. H. J.; Meijer, E. W. *J. Am. Chem. Soc.* **2008**, *130*, 606–611. (e) Stals, P. J. M.; Haveman, J. F.; Martin-Rapun, R. M.; Fitie, C. F. C.; Palmans, A. R. A.; Meijer, E. W. *J. Mater. Chem.* **2009**, *19*, 124–130. (f) Stals, P. J. M.; Smulders, M. M. J.; Martin-Rapun, R.; Palmans, A. R. A.; Meijer, E. W. *Chem. - Eur. J.* **2009**, *15*, 2071–2080. (g) Terashima, T.; Mes, T.; De Greef, T. F. A.; Gillissen, M. A. J.; Besenius, P.; Palmans, A. R. A.; Meijer, E. W. *J. Am. Chem. Soc.* **2011**, *133*, 4742–4745.
- (4) (a) Song, C. E. *Handbook of Asymmetric Heterogeneous Catalysis*; Ding, K. L., Uozumi, Y., Eds.; Wiley-VCH: Weinheim, Germany, 2009; pp 25–72. (b) Zou, H.; Wu, S. S.; Shen, J. *Chem. Rev.* **2008**, *108*, 3893–3957. (c) Minakata, S.; Komatsu, M. *Chem. Rev.* **2009**, *109*, 711. (d) Corma, A. *Chem. Rev.* **1997**, *97*, 2373–2420.
- (5) (a) Lu, J.; Toy, P. H. *Chem. Rev.* **2009**, *109*, 815–838. (b) Trindade, A. F.; Gois, P. M. P.; Afonso, C. A. M. *Chem. Rev.* **2009**, *109*, 418–514. (c) Itsuno, S. *Polymeric Chiral Catalyst Design and Chiral Polymer Synthesis*; Wiley-VCH: Weinheim, Germany, 2011. (d) Itsuno, S.; Hassan, M. M. *RSC Adv.* **2014**, *4*, 52023–52043. (e) Yamamoto, T.; Akai, Y.; Suginome, M. *Angew. Chem., Int. Ed.* **2014**, *53*, 12785–12788. (f) Sun, Q.; Meng, X.; Liu, X.; Zhang, X.; Yang, Y.; Yang, Q.; Xiao, F.-S. *Chem. Commun.* **2012**, *48*, 10505–10507. (g) Xu, X.; Wang, R.; Wan, J.; Ma, X.; Peng, J. *RSC Adv.* **2013**, *3*, 6747–6751. (h) Akai, Y.; Yamamoto, T.; Nagata, Y.; Ohmura, T.; Suginome, M. *J. Am. Chem. Soc.* **2012**, *134*, 11092–11095. (i) Huerta, E.; Stals, P. J. M.; Meijer, E. W.; Palmans, A. R. A. *Angew. Chem., Int. Ed.* **2013**, *52*, 2906–2910.
- (6) (a) Thomas, J. M.; Raja, R. *Acc. Chem. Res.* **2008**, *41*, 708–720. (b) Raja, R.; Thomas, J. M.; Jones, M. D.; Johnson, B. F. G.; Vaughan, D. E. W. *J. Am. Chem. Soc.* **2003**, *125*, 14982–14983. (c) Yang, H. Q.; Zhang, L.; Zhong, L.; Yang, Q. H.; Li, C. *Angew. Chem., Int. Ed.* **2007**, *46*, 6861–6865.
- (7) (a) Liu, R.; Jin, R. H.; An, J. Z.; Zhao, Q. K.; Cheng, T. Y.; Liu, G. H. *Chem. - Asian J.* **2014**, *9*, 1388–1394. (b) Zhang, D. C.; Gao, X. S.; Cheng, T. Y.; Liu, G. H. *Sci. Rep.* **2014**, *4*, 5091. (c) Zhang, D. C.; Xu, J. Y.; Zhao, Q. K.; Cheng, T. Y.; Liu, G. H. *ChemCatChem* **2014**, *6*, 2998–3003. (d) Gao, X. S.; Liu, R.; Zhang, D. C.; Wu, M.; Cheng, T. Y.; Liu, G. H. *Chem. - Eur. J.* **2014**, *20*, 1515–1519. (e) Chen, C.; Kong, L. Y.; Cheng, T. Y.; Jin, R. H.; Liu, G. H. *Chem. Commun.* **2014**, *50*, 10891–10893. (f) Liu, R.; Jin, R. H.; Kong, L. Y.; Wang, J. Y.; Chen, C.; Cheng, T. Y.; Liu, G. H. *Chem. - Asian J.* **2013**, *8*, 3108–3115.
- (8) Mathakiya, I.; Vangani, V.; Rakshit, A. K. *J. Appl. Polym. Sci.* **1998**, *69*, 217–228.
- (9) (a) Wu, X. F.; Li, X. H.; Zanotti-Gerosa, A.; Pettman, A.; Liu, J.; Mills, A. J.; Xiao, J. L. *Chem. - Eur. J.* **2008**, *14*, 2209–2222. (b) Wu, X. F.; Liu, J.; Di Tommaso, D.; Iggo, J. A.; Catlow, C. R.; Bacsa, J.; Xiao, J. L. *Chem. - Eur. J.* **2008**, *14*, 7699–7715. (c) Liu, P. N.; Deng, J. G.; Tu, Y. Q.; Wang, S. H. *Chem. Commun.* **2004**, 2070–2071. (d) Cortez, N. A.; Aguirre, G.; Parra-Hake, M.; Somanathan, R. *Tetrahedron Lett.* **2009**, *50*, 2228–2231.
- (10) Ji, X.; Wang, M. Z.; Ge, X. W.; Liu, H. R. *Langmuir* **2013**, *29*, 1010–1016.
- (11) (a) Zou, H.; Wu, S. S.; Shen, J. *Chem. Rev.* **2008**, *108*, 3893–3957. (b) Nguyen, V.; Yoshida, W.; Cohen, Y. J. *Appl. Polym. Sci.* **2003**, *87*, 300–310.
- (12) (a) Seuring, J.; Agarwal, S. *Macromolecules* **2012**, *45*, 3910–3918. (b) Seuring, J.; Bayer, F. M.; Huber, K.; Agarwal, S. *Macromolecules* **2012**, *45*, 374–384.
- (13) Iyer, B. D.; Mathakiya, I. A.; Shah, A. K.; Rakshit, A. K. *Polym. Int.* **2000**, *49*, 685–690.
- (14) Mao, J.; Baker, D. C. *Org. Lett.* **1999**, *1*, 841–843.
- (15) (a) Zhang, B.; Xu, M. H.; Lin, G. Q. *Org. Lett.* **2009**, *11*, 4712–4715. (b) Phan, D. H. T.; Kim, B.; Dong, V. M. *J. Am. Chem. Soc.* **2009**, *131*, 15608–15609. (c) Murphy, S. K.; Dong, V. M. *J. Am. Chem. Soc.* **2013**, *135*, 5553–5556.